PAPER

Check for updates

An insight into the structure, composition and hardness of a biological material: the shell of freshwater mussels

Anupam Chakraborty,[a] Saida Parveen,[b] Dipak Kr. Chanda [ID] [c] and Gautam Aditya [ID] ⋆[ab]

The shell of the freshwater mussel (Mollusca: Bivalvia) is a composite biological material linked with multifunctional roles in sustaining ecosystem services. Apart from providing mechanical strength and support, the shell is an important site for adherence and growth of multiple types of algae and periphyton. Variations in the shell architecture are observed in the mussels both within a species and among different species. Considering the prospective utility of the shell of the freshwater mussels as a biological material, an assessment of the shell characteristics was accomplished using *Corbicula bensoni* and *Lamellidens marginalis* as model species. The calcium carbonate ($CaCO_3$) content of the shells, physical features and mechanical strength were assessed along with the morphometric analysis. The $CaCO_3$ content of the shell (upto 95% to 96% of the shell weight) of both the mussels was positively correlated with the shell length, suggesting increased deposition of $CaCO_3$ in shells with the growth of the species. The cross sectioned views of FE-SEM images of the shells exhibited distinct layered structure with external periostracum and inner nacreous layer varying distinctly. In the growing region, the growth line was prominent in the mussel shells revealed through the FESEM images. In addition XRD, FTIR and EDS studies on the mussel shells confirmed the existence of both aragonite and calcite forms of the calcium carbonate crystals with the incidence of various functional groups. The mechanical strength of the mussel shells was explored through nanoindentation experiments, revealed significant strength at the nanoparticle level of the shells. It was apparent from the results that the shell of the freshwater mussel *L. marginalis* and *C. bensoni* qualify as a biological material with prospective multiple applications for human well-being and sustaining environmental quality.

1. Introduction

The unique morphological features of all mussels (Mollusca: Bivalvia) is the presence of two symmetrical calcareous valves, constituting the shells, connected by a calcified leathery hinge.[1,2] The toughest calcareous shells of the mussels vary extensively in shape, size, colour and biomass.[3] While calcium carbonate is the dominant chemical constituent of the shells, minor inorganic trace elements are common in different species of bivalves.[3–9] Owing to the presence of the shells with multiple functional attributes, the snails and mussels qualify as ecosystem engineers modifying the constituents and the interactions of the freshwater community.[10–12] Due to the phenotypic variation in traits, the shells of the mussels are vulnerable to the selection process for refinement with higher adaptive value.[13,14] The shell formation in mussels as in other Mollusca, is considered as a typical process of biomineralization;[4,6,15] that may involve the precipitation of the nacreous aragonite from extrapallial fluid reservoirs with prominence of growth bands.[4,16] At a proximate level, the shell formation in snails and mussels involve biodeposition of the ingredient minerals[15] on a biological matrix[17] following different orientation pattern to yield a species specific unique architecture.[3,17] However, the entire process of shell formation is controlled genetically as well as physically at the cellular level.[18–20] The synthesis and remodelling of crystal varieties depend on their thermodynamic stability in the concerned environment.[15,21] Among three forms of $CaCO_3$ crystal, calcite and aragonite forms are more prevalent in constructing the shells of mussels.[5] During the process of shell fabrication, inorganic materials with different shape and size assemble in complex pattern according to various level of hierarchy, and eventually construct the biological material.[22,23]

Varied species of mussels, oysters, and clams are exploited as food resource and therefore bear significance in food security

[a]Department of Zoology, University of Calcutta, 35 Ballygunge Circular Road, Kolkata 700019, India. E-mail: gazoo@caluniv.ac.in; anupambios@gmail.com; Tel: +91-8902595675

[b]Department of Zoology, The University of Burdwan, Golapbag, Burdwan 713104, India. E-mail: parveensaida@gmail.com

[c]Advanced Mechanical and Materials Characterization Division, CSIR-Central Glass and Ceramic Research Institute, Kolkata 700 032, India. E-mail: dipak58c@gmail.com

and livelihood.[12,24] In the natural habitats, in course of the movement and feeding, the mussels facilitate biofiltration,[25,26] bioturbation[27] and biodeposition[28] that enable water purification and nutrient cycling. The mussels and oysters are also the sources for pearl culture.[29–31] Following harvest of mussels from the natural population or from culture, the flesh is extracted (as well as the pearl, if from pearl culture) and the shell is discarded as a waste. The waste shells are highly valued resource used in multiple purposes.[32–36] Owing to a rich source of calcium carbonate, the shells of mussels are converted into useful lime,[37] which can facilitate oil removal[38] or act as a catalyst in biodiesel formation[39,40] or as a catalyst in the 4H pyran formation.[41] The mussel shells can be incorporated in polypropylene[42] or in reinforced composites.[43,44] Application of the whole mussel shell in the sulphate reducing bioreactors for acid mine drainage treatment enables reduction of pollution load.[45] The use of the calcined mussel shell in the waste water treatment is also promoted.[46] A modified mussel shell powder is also used to immobilize microalgae, for removal of nutrients from eutrophic waters.[47] The shells of the mussels are considered as a cheap source of lime and used in mulching the soil[48] that may also induce changes in the pest insect behaviour.[49] Alternatively, the compost bivalve shells can be used, which are more effective than the freshly derived oyster shells.[50] The shells of the mussels and snails are cost effective biosorbent that can be used for the purpose of metal and dye removal,[36,51,52] directly as flakes or granules[53,54] or through the formation of hydroxyapatite.[55] The shells of the bivalves are also considered suitable as fillers and for the use as a substitute to mortar.[56,57] Owing to the diverse applications ranging from the water purification to the soil amelioration, the shells of mussels, oysters and clams are true aquaculture waste with considerable value to safeguard ecology and mobilize economy.

As a potential resource with multiple uses, the characterization of the mussel shells is immensely important to ascertain sustainable use. Exploration of the mussel shell structure enables understanding the functional properties with higher precision that may allow selection as a biological material judiciously. Empirical evidences suggest that the shell characteristics of several mussels, oysters and clams are recorded,[3–9] inclusive of genetic mechanisms of shell protein formation,[18–20] and the calcium carbonate crystal deposition.[6,15,58] Variations in the shell calcium composition and microarchitecture are observed in several studies involving mussels of *Pinctada*, *Pteria*, *Atrenia*, and other genera.[3,7–9,59–61] As a result, the structure of the bivalve shells is well understood through exploration of the crossed lamellar microstructure and nacre layers with aragonite tablets, which provides evidence for its prospective use as biological material.[62] Extending the significance of the mussel shell as a bioresource, an exploration on the microarchitecture, composition and hardness was carried out using the shells of two freshwater mussels, namely *Corbicula bensoni* Deshayes 1854 (Bivalvia: Veneroida) and *Lamellidens marginalis* (Lamarck, 1819) (Bivalvia: Unionoida). On an evolutionary scale, the bivalve families including Unionoida and Veneroida exhibit features to suit the hypoosmotic medium following independent radiations from marine to inland habitats.[2,63] The mussels

under Veneroida (Corbiculidae) and Unionoida are diverse in shape and features, though both are common in freshwater habitats.[1,10] On a proximate scale, the exterior of the shell of *C. bensoni* appears as minute, thin striae and subtrigonal in shape, whereas, the freshwater mussel *L. marginalis* possesses thin, oblong–ovate and roundedly angular shell.[64] An appraisal of the material features remains pre-requisite to promote the utility of the shells of these mussels that are generated as wastes following exploitation for food[65] and pearl.[66,67] Although, the shell dust of *L. marginalis* have shown the potential for bioremediation of heavy metals,[54] the ultrastructural details are yet to be deciphered to suggest their use in other purposes. In the present instance, the shell physical characteristics, chemical composition and the nanomechanical properties were also explored to substantiate the freshwater mussel shells as biological material[68] with prospective application in varied fields as a waste bioresource.[32–36] On the whole, the multifunctionality of the freshwater mussels can be established through the possible use of the waste shells apart from the role in food security and livelihood.

2. Materials and methods

2.1. Preparation of samples

The freshwater mussel *C. bensoni* was collected from Mundeshwari river, Hooghly district, West Bengal, India, during July 2018. At the same time period, the freshwater mussel *L. marginalis* was collected from ponds and lakes in and around Kolkata, West Bengal, India by using insect net of 200 μm mesh size or hand-picked from substratum. Following collection and identification, the flesh of the mussels were removed and the shells were washed under running water and then sun dried.[53,54] Further, the flesh remnant, if any, attached to the shells were removed carefully, prior to the use in the experiments. In order to carry out the characterization of the shells, 23 shells of *C bensoni* and 18 shells of *L. marginalis* were randomly picked from the collections. While selecting the shells, the size differences and the random collections were maintained to qualify each shell as a true replicate. In addition, 23 shells of *C. bensoni* and 16 shells *L. marginalis*, were also used for the determination of the calcium carbonate content. The shell length and shell weight characteristics being – for *C. bensoni* the shell length (SL in mm) ranged between 8.1 mm and 13.7 mm, with mean 10.29 ± 0.35 mm SE, and shell weight (SW, in mg) ranged between 90.6 mg and 256.3 mg, with mean 162.91 ± 11.99 mg SE; for *L. marginalis*, the shell length (SL in mm) ranged between 44.92 mm and 91.01 mm, with mean 74.19 ± 3.5 mm SE, and shell weight (SW, in mg) ranged between 4301.1 mg and 26 380 mg, with mean 13 343.58 ± 1704.1 mg SE. The shell measurements were taken and prepared for the experiments related to the shell surface architecture and nano-scale characterization.[53,54]

2.2. X-ray diffraction (XRD)

Using a mortar and pestle the freshly prepared dry shells were crushed to dust for the XRD analysis. The crystalline phase of

the shell forming major component of shell dust of the two freshwater mussels (*C. bensoni* and *L. marginalis*) were determined by powder XRD analysis, using X'Pert Pro MPD diffractometer (PANalytical, Almelo, The Netherlands). The phase composition data were collected by step wise scanning mode in steps of 0.02° at scattering angles (2θ) ranging from 20° to 80° by using monochromatic Cu-Kα radiation ($\lambda = 1.5406$) at 40 kV and 20 mA.[69]

2.3. Fourier-transform infrared spectroscopy (FTIR)

The study was carried out through mixing 100 mg of KBr containing 1% of dried mussel shell dust (separately for *C. bensoni* and *L. marginalis*), initially. Subsequently, the mixture was ground to form KBr pellets of shell dust for Fourier transform infrared spectrum analysis. The infrared spectrum attributable to the shell dust was obtained in Fourier transform infrared spectrometer (Jasco FT/IR-6300 type A; serial no. A014461024). For both the mussel species, the spectra were collected at a resolution of 4 cm^{-1} with scanning speed of 2 mm per second over a range of 500 to 3500 wave numbers (cm^{-1}).[9,53,70]

2.4. Field-emmission scanning electron microscopy (FESEM) and energy-dispersive X-ray spectroscopy (EDS)

Intact mussels shells were ground into pieces and flat surfaces were chosen to get the images of both inner and outer surfaces. The assessment was made separately for the mussels, *C. bensoni* and *L. marginalis*. In order to access the consecutive inner layers of shells, dilute chemical etching *i.e.* 0.1 (N) HCl was employed for considerable time. As a result, the successive inner shell layers were exposed gradually. Prepared shells were then coated and mounted by using 3 nm thin platinum film and was made ready for FESEM image to insight the surface morphology and consecutive inner layers achieved through acid etching practice by using field-emission scanning electron microscopy (MODEL JEOL JSM-7600F) operated at 15 kV to gain adequate resolution and conductivity for the proper magnification. The EDX measurements of the shells of mussels were performed in INCA Energy 250 Microanalysis System (EDS). The cross-sectioned shell samples were first mounted perpendicularly in a stainless steel mold by using epoxy resin and hardener and the whole system was left for 24 h. After that the resin mounted shell samples were taken out of mold. Subsequently, the samples were grinded and polished by Struers Labopol 5 polishing machine. The surface of the samples were first smoothened by grinding with 240 grit SiC emery paper for 30 seconds at 200 rpm in aforesaid polishing machine, following which the samples were further grinded with 400, 800, 1000 and 1200 grits emery papers respectively to yield smooth surface. After smoothing, the surface was polished by using diamond paste. The resin mounted shell pieces were polished by 9 μm diamond paste in water–glycerol mixture sprayed every 20–30 seconds on napless paper for 5 minutes at 150 rpm in polishing machine. The same procedure was repeated by using 6 μm diamond pastes. Final level of polishing was made by using 1 μm diamond suspended in water-soluble oil and sprayed every 20–30 seconds on napped cloth for 2 minutes at 120 rpm.[71] Finally

mirror finished sample surfaces were obtained. The prepared samples were then mounted directly onto carbon tape for EDX measurement. From the cross sectioned area of each shell sample only the internal mineralized layer was targeted for EDX measurements excluding the outer shell matrix.[21,72,73]

2.5. Determination of nanomechanical properties of biological material

The nanomechanical properties of the shells of *C. bensoni* and *L. marginalis* were evaluated by measuring the nanohardness (H) applying different loads (P) ranges from 100 mN to 700 mN using a Berkovich tip (~radius 150 nm) of a nanoindenter (Fischerscope H100-XYp; Fischer, Switzerland). The loads are applied to the particular position of flat outer surface of the shell samples. All experiments were conducted at room temperature and software generated area function of the indenter tip was applied before each measurement to obtain load (P) *versus* penetration depth (h) data by means of tip blunting effect. The nanoindentation data were analyzed following Oliver and Pharr method.[74]

2.6. Estimation of $CaCO_3$ content in mussel shells

The dried shells following removal of the flesh were subjected to the $CaCO_3$ determination. Prior to the initiation, the shell length (in mg) was determined to the nearest 0.1 mm using a vernier caliper (Insize, Brazil) along with the corresponding shell weight (in mg) to the nearest 0.1 mg, which was measured in a pan balance (Citizen, India). Individual shells of both the mussels, *C. bensoni* and *L. marginalis*, were sequentially subjected to the $CaCO_3$ (in mg) determination. Following measurement, a 2 (M) HCl solution was added in a drop wise manner on the individual shell placed in a beaker and stirred at room temperature until complete digestion of shell occurs. In order to remove the impurities and large particles of shell remnants, the slurry was then filtered through Whatman Grade No. 1 filter paper. Subsequently, to the above filtrate, 2 (M) Na_2CO_3 solution added drop by drop until and unless total precipitation reaction complete to form $CaCO_3$ and sodium chloride.[75] After that the solution cooled to room temperature and to the obtained the $CaCO_3$ precipitate mixture was filtered and then washed to remove soluble salts. The filtered $CaCO_3$ procured from each mussel shell was collected and dried for quantification. A regression equation (along with Pearson's product moment correlation coefficient) was calculated to represent the $CaCO_3$ (in mg) as a function of the shell length and shell weight of the freshwater mussels.

3. Results

3.1. Elemental analysis through EDS, XRD, FTIR pattern study

The comparative XRD patterns of shells of two different mussels (*C. bensoni* and *L. marginalis*) revealed similarities in crystalline peaks (Fig. 1) confirmed the existence aragonite and calcite forms of calcium carbonate. The X-ray diffraction data were composed in steps of 0.02° at scattering angles (2θ) ranging

from 20° to 80°. The XRD phase analysis of aragonite has been revealed in this Fig. 1 having high density peaks at $2\theta = 26.63°$, 29.69°, 33.37°, 36.42°, 38.20°, 43.15°, 46.06°, 48.75°, 52.95° with monochromatic Cu-Kα radiation ($\lambda = 1.5406$). It can be conclude that the shells of two mussels contain aragonite with intense peaks for (111) and (012) planes and calcite with intense peaks for (104) and (202) planes.[9,53,54]

The conformational study about the functional groups was made through FTIR spectra analysis for the shell of two mussels (Fig. 2) which showed similar features. The peak around 2936 cm^{-1} appeared due to the C–H stretching vibration suggestive of the presence of methyl and methylene groups. The spectral peak at 2360 cm^{-1} was due to the COO^{-} functional groups. The band at 1467 cm^{-1} corresponded to the C=C bond and at 1080 cm^{-1} was due to the C–O stretching, which perhaps related the existence of glycosylated proteins of the shell matrix. The characteristic carbonate band at 701.9 cm^{-1}, 713.5 cm^{-1} and 865.8 cm^{-1} revealed the existence of calcium carbonate in the shell.[9,54,69] Identification and classification of different layers of mussel shells were made[21,76–78] accordingly for the interspecific comparison and the variations in the different layers.

3.2. Microstructure observation and characterization with the FESEM

The electron micrographs of the shells of the two mussels *C. bensoni* and *L. marginalis* portrayed three distinct layers in transverse section (Fig. 3A and B) namely, the external protective periostracum layer, the prismatic layer and the inner nacreous layer.

3.2.1. Outer periostracum layer. The protein containing sclerous periostracum layer of the shell of both the mussels was very prominent (Fig. 4A and B). Apparently, the exterior surface of the periostracum of mussel *C. bensoni* shell consisted of prominent, radial, oblique ridges arranged in more or less regular interval. In comparison, the exterior micro ridges were not so prominent but more frequently arranged in the periostracum of the mussel *L. marginalis* with regular folds and corrugations.[5,12] The mild acid etching exposed the inner

Fig. 1 The XRD patterns of the prepared shells of the two freshwater mussels (A) *C. bensoni* and (B) *L. marginalis*. a = intensity peaks for aragonite, c = intensity peaks for calcite.
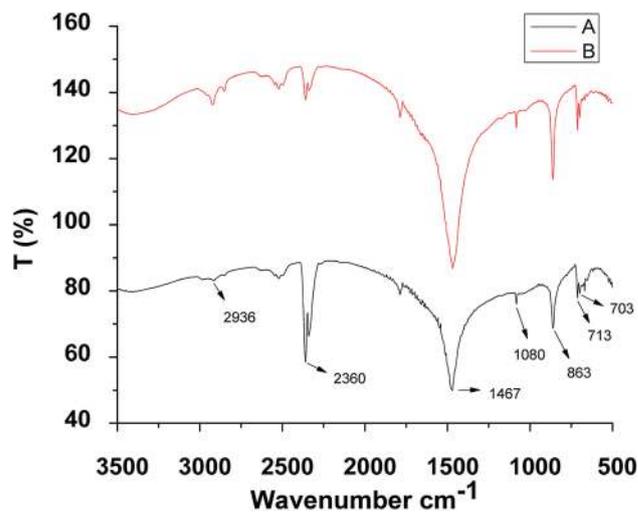

Fig. 2 The representative FTIR spectra of the prepared shells of the two freshwater mussels (A) *C. bensoni* and (B) *L. marginalis*.

vacuolar periostracum which was often continuous with the subsequent inner mineralized layers.[5,72,76,77] The FESEM images (Fig. 4C and D) of inner vesicular layers of the periostracum of the shell of both the mussels showed prominent vacuoles.

3.2.2. Mineralized internal layers. The representations in Fig. 5A and B depict the closed microstructural views of subsequent shell layers of both mussel species. In *C. bensoni*, immediately below periostracum layer inconsistently arranged irregular fibrous prismatic structure was prominent where each prism having common structural nodule (Fig. 5A).[5,72,76,77] Below prismatic layer a distinct cloud layer made up mainly of calcite floating above the nacreous layer. This amorphous supersaturated cloudy structure helps in shell biomineralization. The intersection between calcite layer and adjacent nacreous layer was prominent (Fig. 6A) for *C. bensoni*, while, the nacreous layer where the aragonite made tablets, piled in parallel elongated row stacking manner.[21]

In Fig. 5B, closed view in electron micrograph image of shells of *L. marginalis* illustrates three distinct calcium carbonate layers. Below the periostracum simple aragonite prisms in which the first order columnar prisms, polygonal in shape arranged perpendicular to the outer surface in more or less regular interval. The arrangement pattern of nacreous layer of *L. marginalis* entirely follows the sheet nacre model of nacreous formation (Fig. 6B) in which the individual tablet shaped crystals are somewhat displaced along the succeeding rows to mimic an aggregate of overlapping sheets.[78] In the mussel *L. marginalis*, maximum proportion in the midst of different shell layers was occupied by sheet nacreous layer where the individual aragonite sheets horizontally overlapped with one another to make continuous superimposed sheets (Fig. 6B).[21,76–78] The organization pattern in the growing region of nacreous layer showed distinct growth lines prominent in both species (Fig. 7A and B). With the mineralization and deposition of aragonite plates reorientation and compilation of
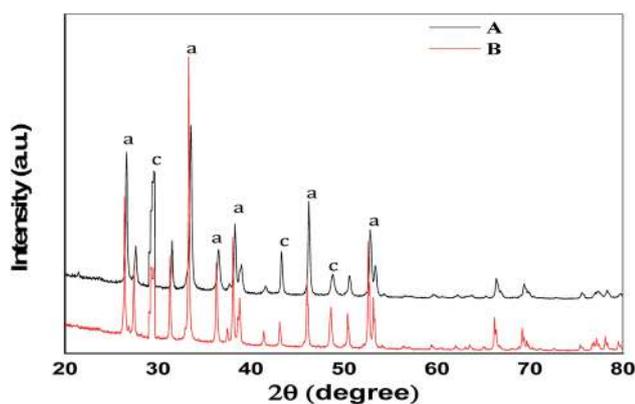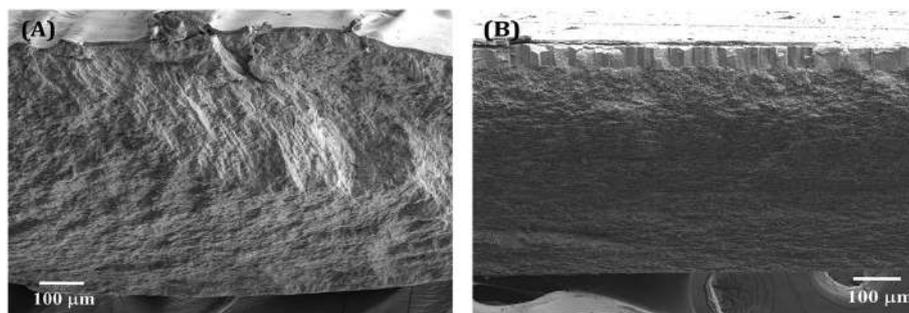
Fig. 3 The cross-sectioned views of shells of (A) *C. bensoni* and (B) *L. marginalis* illustrating different layers. Outer layer is located on the top of the layers.

plates into nacreous sheet proceeded which further surrounded by organic matter to exist as a biocomposite.[3]

3.3. Nanoindentation and mechanical properties of biological materials

The presentation in Fig. 8A and B shows the load (P)–depth (h) plots of the all two mussels shells of *C. bensoni* and *L. marginalis* at different loads (*e.g.*, 100 mN, 300 mN, 500 mN, and 700 mN).[79] From P–h plots it was evident that the final depths of penetrations were the maximum and minimum for the shell samples of *C. bensoni* and *L. marginalis* respectively. So, from P–h plots, it was expected that nanohardness (H) would be minimum for shell of *C. bensoni* and maximum for shell of *L. marginalis*. The nanohardness plot in Fig. 9A and B validates that the maximum hardness was shown by the shell of *L. marginalis* and lower in case of *C. bensoni*. As shown in the figures (Fig. 9A and B), it was evident, that the nanohardness was load independent. This was probably due to layered structures of the

mussel shell.[74,79] The arrangement pattern of calcium carbonate crystal plate in horizontal array was common and clear in the FESEM photomicrograph of each mussel shell sample. Perhaps, this layered structure resulted in the load independency of the nanohardness.[80–82]

3.4. Characterization and estimation of major content of shells of mussels

The EDS spectra of respective mussel shells in Fig. 10A and B confirmed about the elemental composition of mineralized layer. The polymorphs of $CaCO_3$ exhibit strong Ca peaks as well as C and O peaks with the incidence of Mg and Si peaks. Acid digestion of each shell using 2 (M) HCl followed by precipitation reaction by adding 2 (M) Na_2CO_3, calcium carbonate content of individual mussel shell was estimated. The proportion of $CaCO_3$ (in mg) with shell weight (in mg) of the shells of two different mussel species was estimated as: *C. bensoni* (range between 0.51 and 0.98; 0.68 ± 0.04 SE) and *L. marginalis* (range
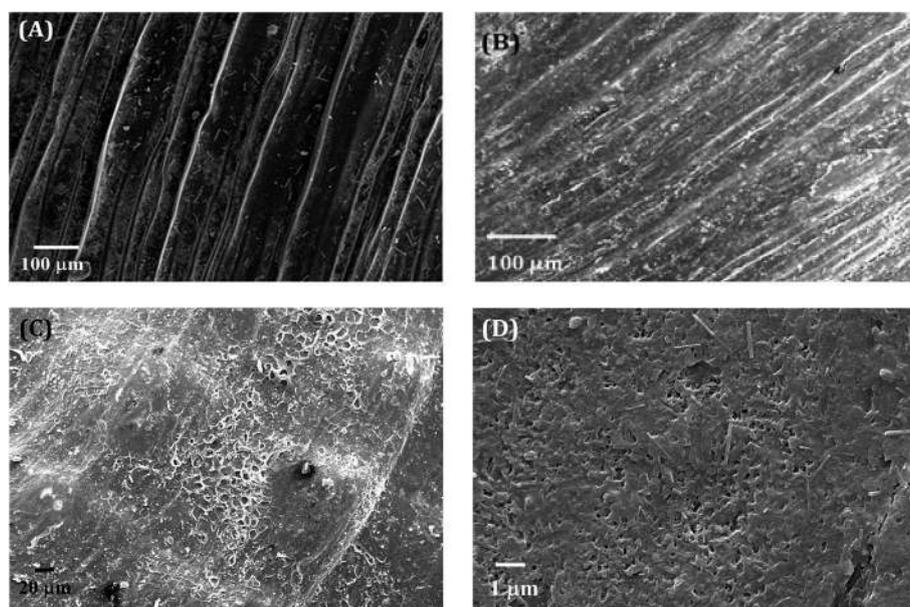

Fig. 4 The most external periostracum is very clear in outer surface of each shell of (A) *C. bensoni* and (B) *L. marginalis*. FESEM images taken after acid-etching of periostracum layers from each shell showing vacuoles in middle periostracum layers of (C) *C. bensoni* and (D) *L. marginalis*.
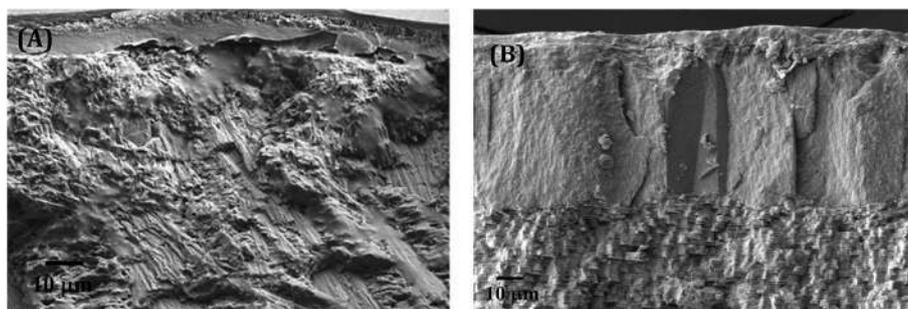
Fig. 5 The FESEM images of close observation on transition zones among different layers within the shells of (A) *C. bensoni* and (B) *L. marginalis*.

between 0.61 and 0.91; mean 0.8 ± 0.03 SE), exhibiting variations with the shell weight considerably. Although the present data support high calcium carbonate content of the shells, the proportional presentation was comparable to freshwater snails that show 95–99.9% calcium carbonate by shell weight with variations in shell size and origin of the snail.[83] For each species the $CaCO_3$ content as a function of shell length complied with a power regression equation ($y = 0.043x^{3.336}$; $r = +0.949$; $r^2 = 0.937$ for *C. bensoni*, $y = 0.693x^{2.218}$; $r = +0.805$; $r^2 = 0.724$ for *L. marginalis*) (Fig. 11A and B). Irrespective of all mussel species, a positive correlation was observed for the correlation between shell weight and $CaCO_3$ content shows power regression equation ($y = 0.430x^{1.065}$; $R^2 = 0.994$) (Fig. 11C). In both instances, the $CaCO_3$ content was observed to be an increasing function of the shell length and shell weight, which indicate that the calcium content in the shells of the mussels vary with the age of the concerned species.[84]

4. Discussion

In the living form, the freshwater mussels carry out several functional roles related to the biofiltration,[25,26] biodeposition,[28] bioturbation[27] and bioremediation,[54] which enable sustenance of the environmental quality.[12] In course of the growth, the addition of mostly the calcium carbonate, increases the biomass of the shell, and therefore makes it more efficient in protecting the living specimen and adds to the quality of the pearl growing inside.[29–31,66,67] However, following harvest of flesh[65] and/or pearl[66,67] the shells are discarded as waste, which bears huge prospect as a biological material.[32–38] While

discarded marine shells derived from mussels, oysters, clams and abalones have been characterized as biological material with multiple utility, few efforts have been made from the freshwater mussels.[41,54] Several studies have shown that shells of marine bivalves and gastropods are more worthy as waste with multiple applications in the field of biodiesel production,[39,40] waste water treatment,[46,47] soil amelioration,[48–50] biosorbent for dye and heavy metal,[45,51,52,54,55] fillers and alternative to mortars,[56,57] and as an alternative to the bone materials.[32] In order to judge and qualify the shells of freshwater mussels as a biological material with potential for multiple applications in agriculture and industry, characterization of the shell at the physical and chemical levels is a pre-requisite. This proposition was justified in the present instance, through the microscopic studies, nanohardness and the chemical characterization of the shells of the two freshwater mussels, *C. bensoni* and *L. marginalis*.

A close observation on the microstructure of the shells of the two common freshwater mussel *C. bensoni* and *L. marginalis* showed variation in construction from the outer periostracum to the inner nacreous layer. The chemical composition with the dominance of the $CaCO_3$, justify that the shells of the mussels as a source and sink of CO_2, thereby bearing significance in the carbon cycle. As the precipitation of the $CaCO_3$ in the shells during the growth and remodeling in the living mussels result in the sequestering of carbon, the shell appears to act as a sink of atmospheric CO_2, which, however, is lost and released in the environment as the shells are degraded naturally. In the snails and mussels, at the cellular level, the genetically and environmentally regulated biomineralization process results in the
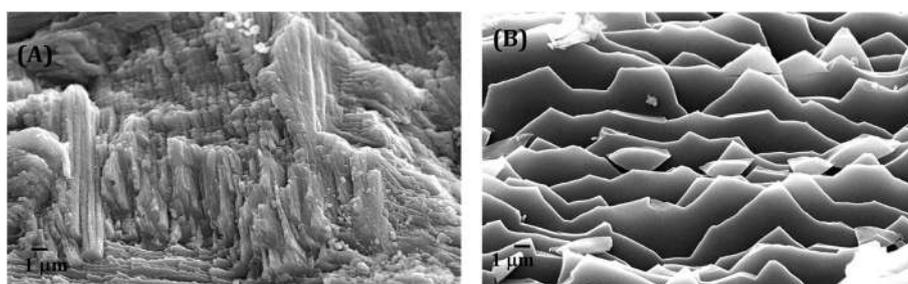

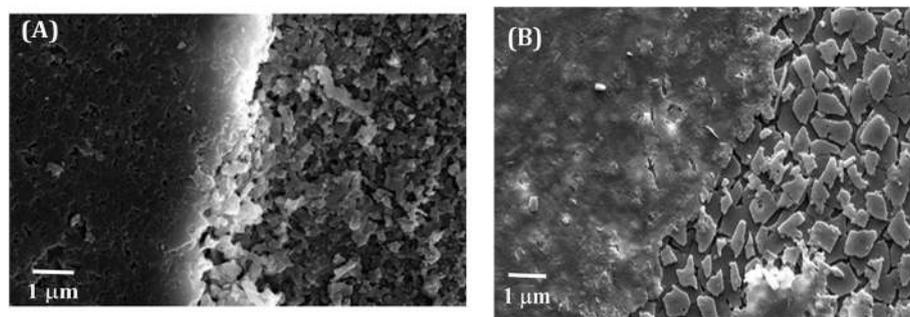**Fig. 6** SEM image of the nacreous layer of the shells of (A) *C. bensoni* and (B) *L. marginalis*.

Fig. 7 The growth front of shell nacre of (A) *C. bensoni* and (B) *L. marginalis*.

distinct shape and form of the shells.[15,18–20] Such variations in the shell shape and shell architecture have been observed in several species reflecting the species specific differences in the shell calcium, mineral and the organic matter contents.

In the present instance, micro-structural divergence in periostracum layers was observed between the two mussel species, reflecting the differences in the regulation and thus disparities in the shape and form of the shells. The sclerotized periostracum containing mainly fibrous protein, carbohydrate and lipids arise from periostracal groove and form a multilayered sculpture.[85] In superficial view, the periostracum of both the mussel species appears smooth and shining in blackish-brown colour.[64] A thin shell with distinct fine striations on periostracum is the distinguishing character of *C. bensoni*. The ridges are not so prominent in central region but are prominent in marginal border of shell in *L. marginalis*. Under FESEM the surface periostracum of the mussel *C. bensoni* exhibit fine ridges arranged obliquely at regular interval whereas in periostracum of the mussel *L. marginalis* micro ridges are not so prominent but regular folds and corrugations are frequent at the marginal area.[5,72,76,77] In addition to the organic matrix layer, crystalline prisms formed the subsequent layer. In *C. bensoni*, the prismatic structure is made up of irregular aragonite fibre to construct common structural module, whereas, simple

aragonite prism fibres compiled into columnar prisms in polygonal shape is very distinct in *L. marginalis*. Variation in fibre length and their orientation are very common and provide significant role in shell growth and remodeling.[86] Amorphous calcite-made cloud layer floating on the nacreous layer helps the shell to increase strength and assist in shell biomineralization.[87,88] There is sharp discrimination in microstructure of nacreous layer of the shells of the two mussel species. Aragonite made tablets piled in row stacking manner arranged parallel to each other to construct the nacreous layer of *C. bensoni*, while, the nacreous layer of *L. marginalis* is arranged as overlapping sheet made up of calcium carbonate crystals. In case of marine mussels (Bivalvia: Pteriidae), the thickness of the nacreous layer vary considerably with reference to different species like *Pinctada martensii*, *Pteria hirundo*, *Atrina pectinata*, *Pteria avicula*, and *Isognomon radiata*.[3] The thickness of the nacreous layer varies from species to species.[3] Adequate thickness with overlapping piling up of the calcium carbonate crystals increase the strength of shell and makes it resistant to fracture.[12] Considering the mussel shells, the nacre appears to be the strongest structure with the fracture strength in bending varying between 35 and 106 MPa (MN^{m-2}) as observed for wide range of bivalve species[89] supported by further studies on the mussel *Pinctada margaritifera*, with a value of 210 MPa.[59] A separate study also
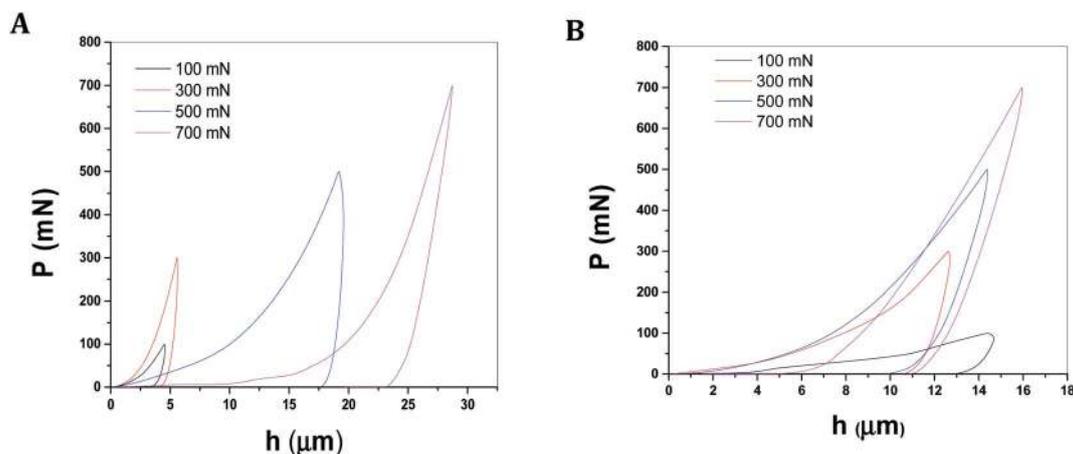

Fig. 8 Typical load depth (*P*–*h*) plots from nanoindentation experiments conducted on biological materials like shells of mussels (A) *C. bensoni* and (B) *L. marginalis*.
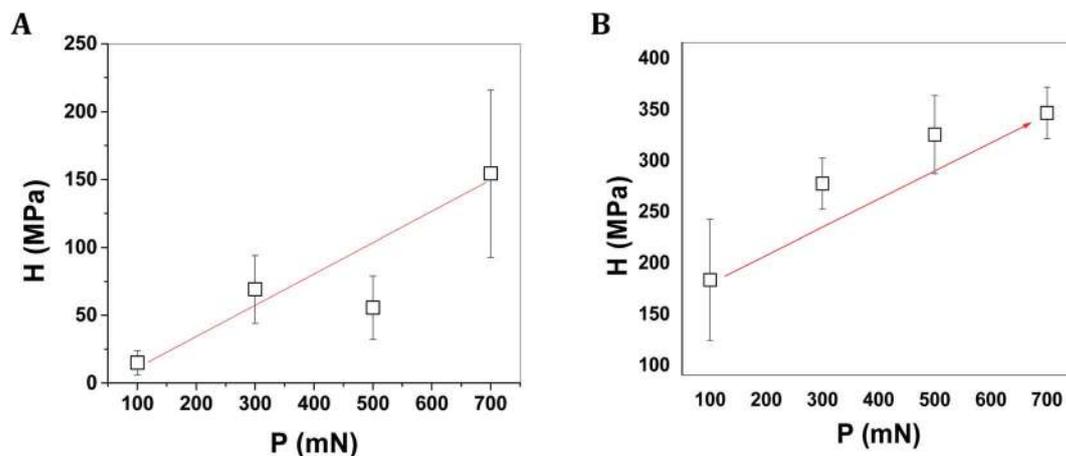
Fig. 9 The variation of nanohardness of shells of mussels (A) *C. bensoni* and (B) *L. marginalis* as a function of load applied in nanoindentation test on shell samples.
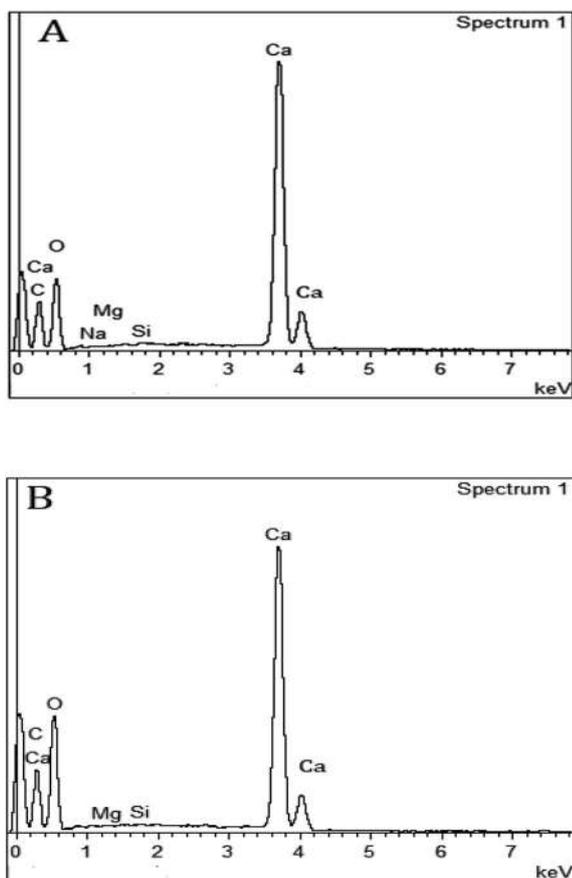

Fig. 10 The SEM-EDS of cross sectioned surface of shells (A) *C. bensoni* and (B) *L. marginalis*.

substantiated the tensile strength of the nacre of *Pinctada* to between 140 MPa and 170 MPa for wet and dry condition of the shell respectively[60] with corresponding Young modulus being 70 GPa and 60 GPa. Assuming correlations between tensile strength and nanoindentation properties,[90] the present data appear to be similar with the tensile strength could be deduced for *C. bensoni* and *L. marginalis*, but considerably low than red abalone, where the tensile strength to be greater than 170 MPa.

The growth and structural flexibility of biological materials depend mainly on the favourable interactions among various organic molecules. In this case, orientation and assemblage of crystal faces on stretched matrix bed remains essential to construct different layers of mussel shells. Unique crystalline property of aragonite and calcite in maintaining constructional flexibility is evident through different studies.[91–93] Aragonite form of crystal is much harder and relatively less brittle than that of other forms of calcium carbonate crystals like vaterite and calcite and show versatility in bonding with other elements. This makes the aragonite composing shell mechanically more stable than the other forms. On the other hand, the calcite made layers in shells are structurally more strong and their arrangement patterns are energetically more favourable.[94–97] Although aragonite and the calcite forms are redundant in the mussel shells, the amount vary with the size of shells as observed in *Mytilus trossulus* from Gulf of Gdansk, Poland.[84] The aragonite content varied with the shell height (shell length) of *M. trossulus* ranging between ~24% for the smaller size class to the 35% for the largest size class. In the present instance, the calcium carbonate content increased with the corresponding increase in the shell length and shell weight of both the species. These physical and chemical attributes enable the shells of the freshwater mussel *C. bensoni* and *L. marginalis* to qualify as unique biological materials for multiple applications (Fig. 12) beyond the level of heavy metal bioremediation.[54] Considering the potential multiple uses of the shells of the freshwater mussels, exploration in the characterization of the shells of different species seems obvious. The recognition of the potential uses of the shell of freshwater mussels would add importance as a biological resource with valued ecosystem service provider.[12]
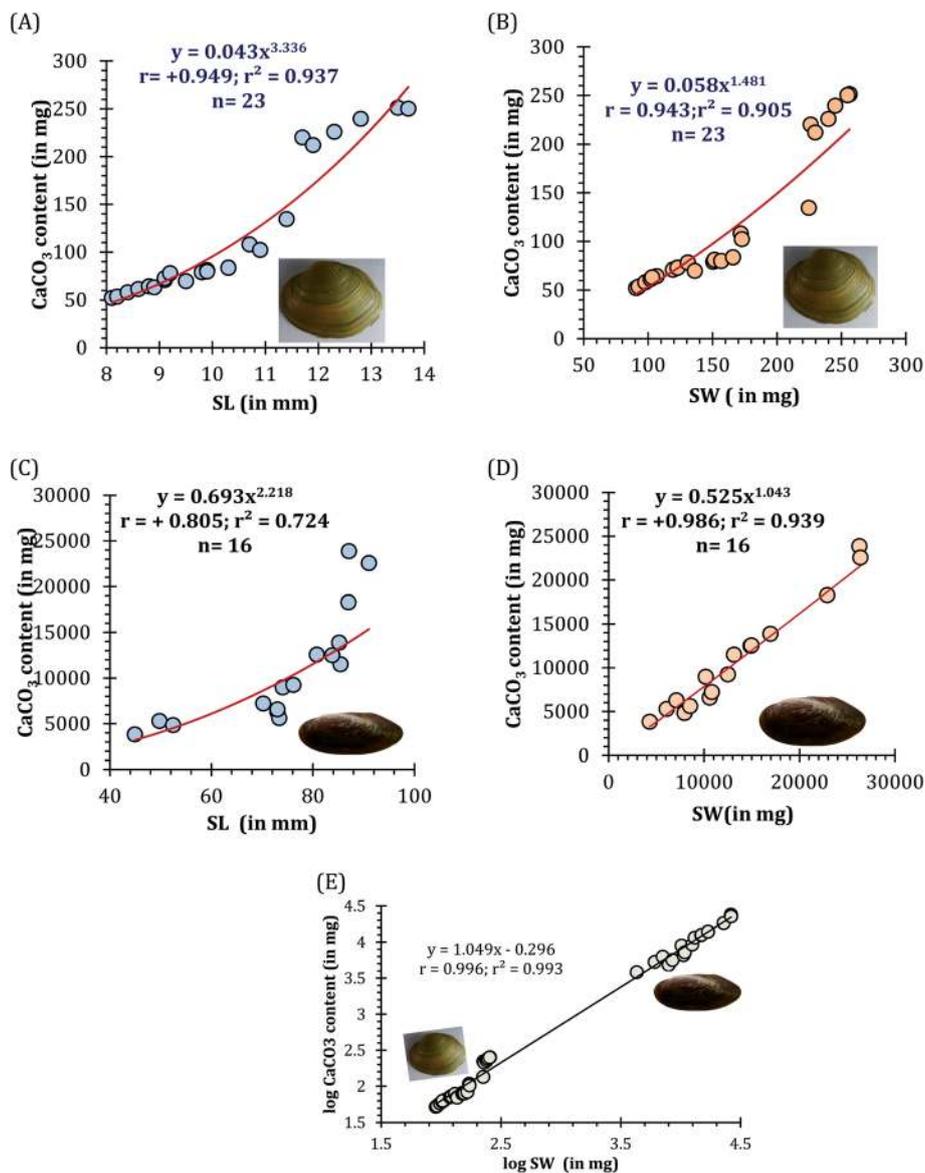
Fig. 11 The calcium content (in mg) in both the freshwater mussel species *C. bensoni* and *L. marginalis*. Here, (A) $CaCO_3$ (in mg) as a function of shell length (SL, in mm) and (B) as a function of shell weight (SW, in mg) of *C. bensoni*, while (C) $CaCO_3$ (in mg) as a function of shell length (SL, in mm) and (D) as a function of shell weight (SW, in mg) of *L. marginalis* and (E) correspondence of the shell weight (log SW, in mg) and $CaCO_3$ content (in mg) (log transformed value), irrespective of species.

5. Conclusion

The diverse arrangement pattern of calcite and aragonite crystals in different layer of the shell of two freshwater mussels *C. bensoni* and *L. marginalis* form distinct structures like fibrous prismatic structure, distinct calcite made cloud layer, sheet like nacreous layer, which make the shells mechanically tough and tensile. The microstructure of shells showed uniformity in the surface architecture and regular arrangement pattern of crystal fibre along its entire framework. The shells having particular high mineral content confirm unusually good mechanical performance as a biological material. Through the process of biomineralization, growth and remodelling the mussel shells construct layered pattern of crystalline aggregates that confirms both structural and functional adaptability with stability to ensure the structural hierarchy.[72] In course of addition of the calcium carbonate in the shell, for growth, repair and remodelling, the mussels influence the global carbon cycle involving carbon dioxide and bicarbonates that seemed to vary with the size of the shell. Considering the calcium content and integrity at the nanoscale, the shells can serve as biosorbent and thereby involve in the removal of the dyes and heavy metal from the freshwater ecosystem. The similarity in the chemical composition and structural organization of the shells of *C. bensoni* and *L. marginalis* with the marine mussels, oysters and clams, indicate that the shell derived materials can be used for multiple purposes including, amelioration of the soil condition, reduction of eutrophication, waste water purification, catalyst
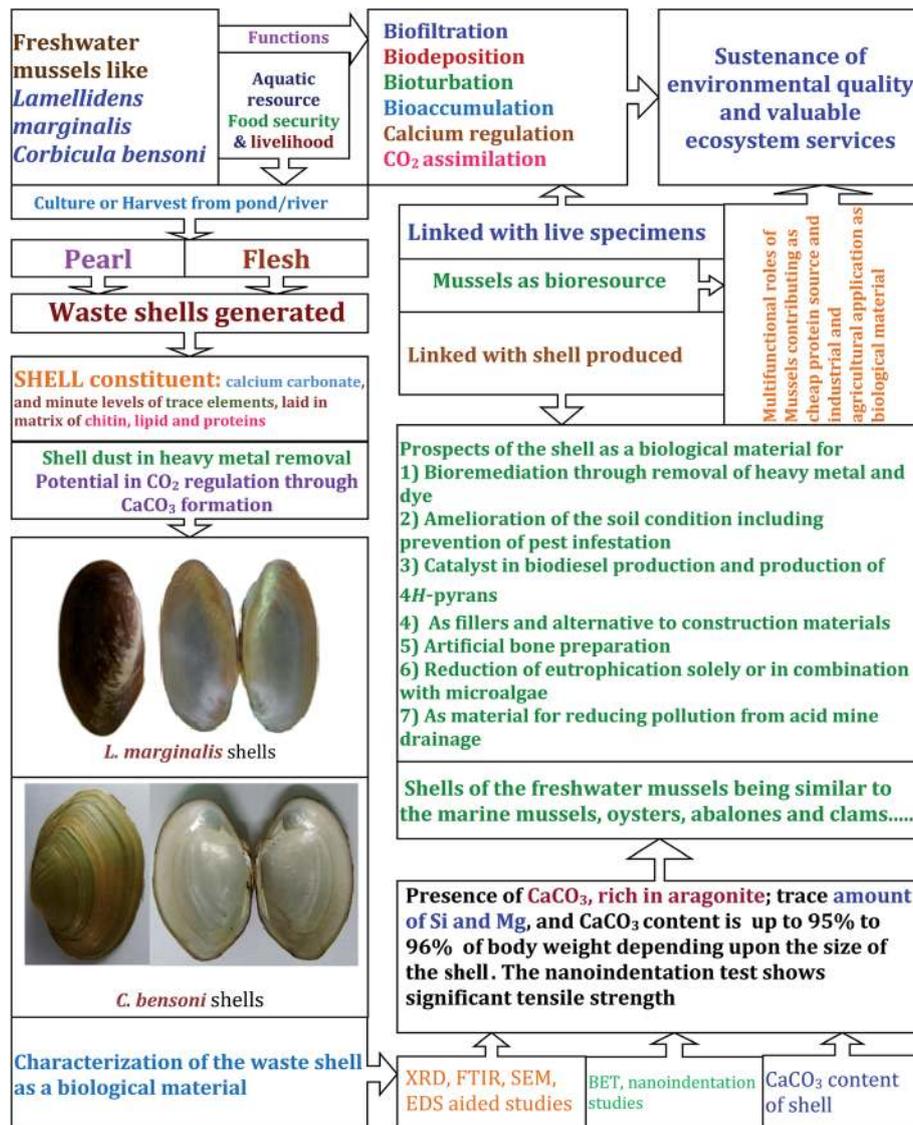
Fig. 12 The schematic representation highlights the functional roles of living freshwater mussels and the contributions of the shells in the sustenance of ecosystem service. As a part of bioprospecting the shells, discarded from aquaculture or otherwise, the material characteristics was evaluated, which substantiated the significance of freshwater mussel shells as biological material with multiple uses.

in biodiesel production and as fillers and construction substitutes. Further possibilities of the use of the nano-scale shell particles in environmental bioremediation can be carried out to prove the cost effectiveness of the biological material.

Conflicts of interest

There are no conflicts to declare.

Acknowledgements

References

1 A. E. Bogan, *Hydrobiologia*, 2008, **595**, 139–147.

2 D. L. Graf, *Am. Malacol. Bull.*, 2013, **31**, 135–153.

3 A. G. Checa, T. Okamoto and J. Ramírez, *Proc. R. Soc. London, Ser. B*, 2006, **273**, 1329–1337.

4 M. Carroll and C. S. Romanek, *Geo-Mar. Lett.*, 2008, **28**, 369–381.

5 A. Nakamura-Filho, A. C. D. Almeida, H. E. Riera, J. L. F. D. Araújo, V. J. P. Gouveia, M. D. D. Carvalho and A. V. Cardoso, *Mater. Res.*, 2014, **17**, 15–22.

6 N. Spann, E. M. Harper and D. C. Alridge, *Naturwissenschaften*, 2010, **97**, 743–751.

7 O. B. Agbaje, I. B. Shir, D. B. Zax, A. Schmidt and D. E. Jacob, *Acta Biomater.*, 2018, **80**, 176–187.

8 O. B. Agbaje, D. E. Thomas, J. G. Dominguez, B. V. Mclnerney, M. A. Kosnik and D. E. Jacob, *J. Mater. Sci.*, 2019, **54**, 4952–4969.

9 O. B. Agbaje, R. Wirth, L. F. G. Morales, K. Shirai, M. Kosnik, T. Watanabe and D. E. Jacob, *R. Soc. Open Sci.*, 2017, **4**, 170622.

10 A. G. Bogan and K. J. Roe, *J. North Am. Benthol. Soc.*, 2008, **27**(2), 349–369.

11 M. Lopes-Lima, L. E. Burlakova, A. Y. Karatayev, K. Mehler, M. Seddon and R. Sousa, *Hydrobiologia*, 2018, **810**, 1–14.

12 C. C. Vaughn, *Hydrobiologia*, 2018, **810**, 15–27.

13 M. Shimamoto, *Sci. Rep. Tohoku Univ., Ser. 2*, 1986, **56**, 1–39.

14 D. Chateigner, C. Hedegaard and H. R. Wenk, *J. Struct. Geol.*, 2000, **22**, 1723–1735.

15 F. Marin, N. L. Roy and B. Marie, *Front. Biosci.*, 2012, **4**, 1099–1125.

16 R. J. Neves and S. N. Moyer, *Am. Malacol. Bull.*, 1988, **6**, 179–188.

17 B. Marie, J. Arivalagan, L. Mathéron, G. Bolbach, S. Berland, A. Marie and F. Marin, *J. R. Soc., Interface*, 2016, **14**, 20160846.

18 X. Wang, L. Li, Y. Zhu, Y. Du, X. Song, Y. Chen, R. Huang, H. Que, X. Fang and G. Zhang, *PLoS One*, 2013, **8**(6), e66522.

19 A. K. Hüning, S. M. Lange, K. Ramesh, D. E. Jacob, D. J. Jackson, U. Panknin, M. A. Gutowska, E. E. R. Philipp, P. Rosenstiel, M. Lucassen and F. Melzner, *Mar. Genom.*, 2016, **27**, 57–67.

20 K. Ramesh, T. Yarra, M. S. Clark, U. John and F. Melzner, *Ecol. Evol.*, 2019, **9**, 7157–7172.

21 J. G. Carter, P. J. Harries, N. Malchus, A. F. Sartori, L. C. Anderson, R. Bieler, A. E. Bogan, E. V. Coan, J. C. Cope, S. Cragg and J. Garcia-March, *Treatise Online*, 2012, **48**, 1–209.

22 L. Li, X. Zhang, H. Yun and G. Li, *Sci. Rep.*, 2017, **7**, 1935.

23 X. Li, W.-C. Chang, Y. J. Chao, R. Wang and M. Chang, *Nano Lett.*, 2004, **4**(4), 613–617.

24 F. M. Suplicy, *Rev. Aquacult.*, 2020, **12**, 204–223.

25 A. Binelli, S. Magni, C. Soave, F. Marazzi, E. Zuccato, S. Castiglioni, M. Parolini and V. Mezzanotte, *Ecol. Eng.*, 2014, **71**, 710–721.

26 E. Voudanta, K. A. Kormas, S. Monchy, A. Delegrange, D. Vincent, S. Genitsaris and U. Christaki, *PeerJ*, 2016, **4**, e1829.

27 B. R. Smith, D. C. Aldridge and A. J. Tanentzap, *Sci. Total Environ.*, 2018, **622–623**, 49–56.

28 P. Bergström, N. Hällmark, K.-J. Larsson and M. Lindegarth, *Aquacult. Int.*, 2019, **27**, 89–104.

29 S. J. Preston, A. Keys and D. Roberts, *Aquat. Conserv.*, 2007, **17**(5), 539–549.

30 C. E. Lind, B. S. Evans, J. Knauer, J. J. U. Taylor and D. R. Jerry, *Aquaculture*, 2009, **286**, 12–19.

31 M. P. Gosselin, *Limnologica*, 2015, **50**, 58–66.

32 Z. Yao, M. Xia, H. Li, T. Chen, Y. Ye and H. Zheng, *Crit. Rev. Environ. Sci. Technol.*, 2014, **44**, 2502–2530.

33 Y. Hou, A. Shavandi, A. Carne, A. A. Bekhit, T. B. Ng, R. C. F. Cheung and A. E. A. Bekhit, *Crit. Rev. Environ. Sci. Technol.*, 2016, **46**, 1047–1116.

34 J. P. Morris, T. Backeljau and G. Chapelle, *Rev. Aquacult.*, 2019, **11**(1), 42–57.

35 A. Hart, *Waste Manage. Res.*, 2020, **38**(5), 514–527.

36 S. Tamjedi and A. Ameri, *Environ. Sci. Pollut. Res.*, 2020, **27**, 31105–31119.

37 M. C. Barros, P. M. Bello, M. Bao and J. J. Torrado, *J. Cleaner Prod.*, 2009, **17**, 400–407.

38 D. Wei, H. Zhang, L. Cai, J. Guo, Y. Wang, L. Ji and W. Song, *Materials*, 2018, **11**(8), 1410.

39 S. Hu, Y. Wang and H. Han, *Biomass Bioenergy*, 2011, **35**, 3627–3635.

40 A. Perea, T. Kelly and Y. Hangun-Balkir, *Green Chem. Lett. Rev.*, 2016, **9**(1), 27–32.

41 U. P. Patil, R. C. Patil and S. S. Patil, *React. Kinet., Mech. Catal.*, 2020, **129**, 679–691.

42 M. R. R. Hamester, P. S. Balzer and D. Becker, *Mat. Res.*, 2012, **15**(2), 204–208.

43 C. Koçhan, *Mater. Test.*, 2019, **61**, 149–154.

44 C. Koçhan, *Mater. Res. Express*, 2019, **6**, 085105.

45 B. Uster, A. D. O'Sullivan, S. Y. Ko, A. Evans, J. Pope, D. Trumm and B. Caruso, *Mine Water Environ.*, 2015, **34**, 442–454.

46 M. Jones, L. Wang, A. Abeynaike and P. Darrell, *Adv. Appl. Ceram.*, 2011, **110**, 280–286.

47 L. Ji, W. Song, D. We, D. Jiang, L. Cai, Y. Wang, J. Guo and H. Zhang, *Bioresour. Technol.*, 2019, **284**, 36–42.

48 E. Álvarez, M. J. Fernández-Sanjurjon, N. Seco and S. Núñez, *Pedosphere*, 2012, **22**(2), 152–164.

49 M. González-Chang, S. Boyer, G. L. Creasy, M.-C. Lefort and S. D. Wratten, *Agron. Sustainable Dev.*, 2017, **37**, 42.

50 Y. H. Lee, S. M. A. Islam, S. J. Hong, K. M. Cho, K. R. K. Math, J. Y. Heo, H. Kim and H. D. Yun, *Biosci., Biotechnol., Biochem.*, 2010, **74**(8), 1517–1521.

51 C. A. Papadimitriou, G. Krey, N. Stamatis and A. Kallianiotis, *J. Chem. Technol. Biotechnol.*, 2017, **92**(8), 1943–1947.

52 H. Delali, D. R. Merouani, H. Aguedal, M. Belhakem, A. Iddou and B. Ouddane, *Key Eng. Mater.*, 2019, **800**, 187–192.

53 A. Hossain and G. Aditya, *J. Environ. Chem. Eng.*, 2013, **1**, 574–580.

54 A. Hossain, S. R. Bhattacharyya and G. Aditya, *ACS Sustainable Chem. Eng.*, 2015, **3**, 1–8.

55 S. Meski, N. Tazibt, H. Khireddine, S. Ziani, W. Biba, S. Yala, D. Sidane, F. Boudjouan and N. Moussaoui, *Water Sci. Technol.*, 2019, **80**(7), 1226–1237.

56 H. Yoon, S. Park, K. Lee and J. Park, *Waste Manage. Res.*, 2004, **22**(3), 158–170.

57 A. Edalat-Behbahani, F. Soltanzadeh, M. Emam-Jomeh and Z. Soltan-Zadeh, *European Journal of Environmental and Civil Engineering*, 2019, DOI: 10.1080/19648189.2019.1607780.

58 L. W. Fritz, L. M. Ragone, R. A. Lutz and S. Swapp, *Limnol. Oceanogr.*, 1990, **35**(3), 756–762.

59 J. D. Currey, P. Zioupos, D. Peter and A. Casinos, *Proc. R. Soc. London, Ser. B*, 2001, **268**, 107–111.

60 A. P. Jackson, J. F. V. Vincent and R. M. Turner, *Proc. R. Soc. London, Ser. B*, 1988, **234**, 415–440.

61 M. J. Almeida, L. Pereira, C. Milet, J. Haigle, M. Barbosa and E. Lopez, *J. Biomed. Mater. Res.*, 2001, **57**, 306–312.

62 M. A. Meyers, A. Y.-M. Lin, P.-Y. Chen and J. Muyco, *J. Mech. Behav. Biomed. Mater.*, 2008, **1**, 76–85.

63 I. Kobayashi, *Am. Zool.*, 1969, **9**, 663–672.

64 N. V. Subba Rao, *Handbook freshwater molluscs of India*, Zoological Survey of India, Calcutta, 1989.

65 A. Haldar, T. K. Dey, P. Dhar and J. Chakrabarti, *IOSR J. Environ. Sci., Toxicol. Food Technol.*, 2014, **8**(8), 1–7.

66 S. K. Raut and A. Biswas, *Basteria*, 1989, **53**, 105–109.

67 K. Janakiram, *J. Appl. Aquacult.*, 2003, **13**(3–4), 341–349.

68 M. A. Meyers, P.-Y. Chen, A. Y.-M. Lin and Y. Seki, *Prog. Mater. Sci.*, 2008, **53**, 1–206.

69 C. E. Weir and E. R. Lippincott, *J. Res. Natl. Bur. Stand.*, 1961, **65**, 173–183.

70 M. Ni and B. D. Ratner, *Surf. Interface Anal.*, 2008, **40**, 1356–1361.

71 R. E. Chinn, *Ceramography: Preparation and Analysis of Ceramic Microstructures*, ASM International, Materials Park, Ohio, USA, 2002.

72 C. T. Callil and M. C. Mansur, *Rev. Bras. Zool.*, 2005, **22**, 724–734.

73 A. E. Tanur, N. Gunari, R. M. Sullan, C. J. Kavanagh and G. C. Walker, *J. Struct. Biol.*, 2010, **169**, 145–160.

74 P. G. Allison, J. M. Seiter, A. Diaz, J. H. Lindsay, R. D. Moser, R. V. Tappero and A. J. Kennedy, *J. Mech. Behav. Biomed. Mater.*, 2016, **53**, 142–150.

75 N. Rungpin, S. Pavasupree, P. Prasassarakich and S. Poompradub, *Polym. Compos.*, 2015, **36**, 1620–1628.

76 J. G. Carter, Evolutionary significance of the shell microstructure in the Paleotaxodonta, Pteriomorpha and Isofilibranchia (Mollusca: Bivalvia), in *Skeletal biomineralization: patterns, processes and evolutionary trends*, ed. J. G. Carter, 1990, vol. 1, pp. 135–296.

77 J. G. Carter, K. Bandel, V. de Buffrénil, S. J. Carlson, J. Castanet, M. A. Crenshaw, J. E. Dalingwater, H. Francillon-Vieillot, J. Géraudie, F. J. Meunier, H. Mutvei,

A. de Ricqlès, J. Y. Sire, A. B. Smith, J. Wendt, A. Williams and L. Zylberberg, Glossary of skeletal biomineralization, in *Skeletal biomineralization: patterns, processes and evolutionary trends*, ed. J. G. Carter, 1990, vol. 1, pp. 609–671.

78 S. M. de Paula and M. Silveira, *Micron*, 2009, **40**, 669–690.

79 D. K. Chanda, S. R. Chowdhury, M. Bhattacharya, A. K. Mandal, N. Dey and A. K. Mukhopadhyay, *Constr. Build. Mater.*, 2018, **158**, 516–534.

80 C. Bignardi, M. Petraroli and N. M. Pugno, *J. Nanosci. Nanotechnol.*, 2010, **10**, 6453–6460.

81 T. P. Sathishkumar, S. Satheeshkumar and J. Naveen, *J. Reinf. Plast. Compos.*, 2014, **33**, 1258–1275.

82 P. S. Das, M. Bhattacharya, D. K. Chanda, S. Dalui, S. Acharya, S. Ghosh and A. K. Mukhopadhyay, *J. Phys. D: Appl. Phys.*, 2016, **49**, 235503.

83 M. M. White, M. Chejlava, B. Fried and J. Sherma, *Am. Malacol. Bull.*, 2007, **22**, 139–142.

84 A. Piwoni-Piórewicz, P. Kukliński, S. Strekopytov, E. Humphreys-Williams, J. Najorka and A. Iglikowska, *Environ. Monit. Assess.*, 2017, **189**, 197.

85 B. Farre, A. Brunelle, O. Laprévote, J. P. Cuif, C. T. Williams and Y. Dauphin, *Comp. Biochem. Physiol., Part B: Biochem. Mol. Biol.*, 2011, **159**, 131–139.

86 Y. Dauphin, G. Luquet, M. Salome, L. Bellot-Gurlet and J. P. Cuif, *J. Microsc.*, 2018, **270**, 156–169.

87 M. Frenzel and E. M. Harper, *J. Struct. Biol.*, 2011, **174**, 321–332.

88 S. W. Lee and C. S. Choi, *Cryst. Growth Des.*, 2007, **7**, 1463–1468.

89 J. D. Currey, *Proc. R. Soc. London, Ser. B*, 1977, **196**, 443–463.

90 R. Rodriguez and I. Gutierrez, *Mater. Sci. Eng., A*, 2003, **361**(1–2), 377–384.

91 M. G. Willinger, A. G. Checa, J. T. Bonarski, M. Faryna and K. Berent, *Adv. Funct. Mater.*, 2016, **26**, 553–561.

92 W. L. Roberts, G. R. Rapp Jr and J. Weber, *Encyclopaedia of Minerals*, Van Nostrand Reinhold, New York, 1974.

93 J. D. Taylor and D. G. Reid, *Hydrobiologia*, 1990, **193**, 199–215.

94 G. Falini, S. Albeck, S. Weiner and L. Addadi, *Science*, 1996, **271**, 67–69.

95 D. E. Jacob, A. L. Soldati, R. Wirth, J. Huth, U. Wehrmeister and W. Hofmeister, *Geochim. Cosmochim. Acta*, 2008, **72**, 5401–5415.

96 L. Chauvaud, J. K. Thompson, J. E. Cloern and G. Thouzeau, *Limnol. Oceanogr.*, 2003, **48**, 2086–2092.

97 E. Harper, *Paleontology*, 1977, **40**, 71–97.